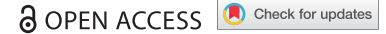







RESEARCH PAPER



# Comprehensive search for accessory proteins encoded with archaeal and bacterial type III CRISPR-*cas* gene cassettes reveals 39 new *cas* gene families

Shiraz A. Shah <sup>a,d,\*</sup>, Omer S. Alkhnbashi<sup>b\*</sup>, Juliane Behler<sup>c</sup>, Wenyuan Han <sup>d</sup>, Qunxin She <sup>d</sup>, Wolfgang R. Hess <sup>c,e</sup>, Roger A. Garrett<sup>d</sup>, and Rolf Backofen <sup>b,f</sup>

<sup>a</sup>Copenhagen Prospective Studies on Asthma in Childhood, Herlev and Gentofte Hospital, University of Copenhagen, Denmark; <sup>b</sup>Freiburg Bioinformatics Group, Department of Computer Science, University of Freiburg, Freiburg, Germany; <sup>c</sup>Genetics and Experimental Bioinformatics, Faculty of Biology, University of Freiburg, Freiburg, Germany; <sup>d</sup>Danish Archaea Centre, Department of Biology, University of Copenhagen, Copenhagen N, Denmark; <sup>e</sup>Freiburg Institute for Advanced Studies, University of Freiburg, Freiburg, Germany; <sup>f</sup>BIOSS Centre for Biological Signaling Studies, University of Freiburg, Freiburg, Germany

## ABSTRACT

A study was undertaken to identify conserved proteins that are encoded adjacent to *cas* gene cassettes of Type III CRISPR-Cas (Clustered Regularly Interspaced Short Palindromic Repeats – CRISPR associated) interference modules. Type III modules have been shown to target and degrade dsDNA, ssDNA and ssRNA and are frequently intertwined with cofunctional accessory genes, including genes encoding CRISPR-associated Rossman Fold (CARF) domains. Using a comparative genomics approach, and defining a Type III association score accounting for coevolution and specificity of flanking genes, we identified and classified 39 new Type III associated gene families. Most archaeal and bacterial Type III modules were seen to be flanked by several accessory genes, around half of which did not encode CARF domains and remain of unknown function. Northern blotting and interference assays in *Synechocystis* confirmed that one particular non-CARF accessory protein family was involved in crRNA maturation. Non-CARF accessory genes were generally diverse, encoding nuclease, helicase, protease, ATPase, transporter and transmembrane domains with some encoding no known domains. We infer that additional families of non-CARF accessory proteins remain to be found. The method employed is scalable for potential application to metagenomic data once automated pipelines for annotation of CRISPR-Cas systems have been developed. All accessory genes found in this study are presented online in a readily accessible and searchable format for researchers to audit their model organism of choice: <http://accessory.crispr.dk>.

## ARTICLE HISTORY

Received 13 February 2018  
Accepted 12 May 2018

## KEYWORDS



CRISPR; *cas*; archaea; bacteria; type III; accessory; auxiliary; ancillary; CARF; *csx1*; *csx3*; nuclease; protease; helicase

## 1. Introduction


Type III CRISPR-Cas systems have been classified into four main subtypes A to D of which subtypes III-A and III-B have been studied extensively [1,2]. They often coexist within cells carrying Type I systems and are assumed to complement the latter functionally. However, whereas Type I systems specifically target dsDNA, Type III systems can degrade dsDNA, ssDNA and ssRNA [3–9]. Importantly, an earlier survey of archaeal *cas* gene cassettes revealed that Type III modules are exceptional in that they frequently carry accessory genes either within or immediately bordering their core *cas* gene modules [1]. Some of these accessory genes encode putative proteases or nucleases suggesting that they provide additional functions that modulate, complement or extend, Type III interference functions.

Some accessory *cas* genes were initially identified during the first comprehensive CRISPR-Cas subtype classification [10]. Core *cas* genes were found to be conserved across most CRISPR-Cas subtypes, while a different class of *cas* genes

displayed a more variable distribution and were not consistently associated with specific subtypes. Such genes were designated *csx* and six gene families, *csx1*–6, were classified [10]. In the next major CRISPR-Cas systematics update, some accessory *cas* gene families were merged into the existing, and new, core *cas* gene families, with only the *csx1* and *csx3* families remaining separate [11]. This more robust definition of core *cas* gene families enabled a more rigorous distinction to be made from eventual new accessory genes. Building on this, an archaea-specific study identified almost twenty new *cas* accessory gene families that were considered distinct from core *cas* gene families, an inference that was reinforced by their variable distribution amongst CRISPR-Cas subtypes [1]. Most of the accessory genes were found to be associated with Type III systems, and most of the encoded proteins were related to the original *Csx1* family proteins [10]. Two additional Type III subtypes, III-C and III-D were also introduced, and they were seen to be associated with many of the same accessory genes as those linked to Type III-A and III-B modules [1]. Later, the *Csx1* protein family was formally defined

**CONTACT** Rolf Backofen  [backofen@informatik.uni-freiburg.de](mailto:backofen@informatik.uni-freiburg.de)  Freiburg Bioinformatics Group, Department of Computer Science, University of Freiburg, Georges-Köhler-Allee 106 79110, Freiburg, Germany

\*The authors share the first authorship

 Supplemental data for this article can be accessed [here](#).

by its ligand binding CARF domain and was annotated in both archaea and bacteria [12]. In addition, a few bacterial accessory protein families lacking CARF domains were found and added to the TIGRFAMs database by an author of the original study [10]. The latest CRISPR-Cas systematics update [2] adopted the new Type III subtypes and integrated many of the newly identified archaeal and bacterial accessory gene families. Moreover, subtype III-D was extended to include disparate bacterial Type III systems that had previously defied classification. As a result, their core genes were relatively poorly characterized and were sometimes annotated as accessory genes. Nevertheless, Makarova et al. (2015)[12] provided detailed annotations of all known archaeal and bacterial CRISPR-Cas systems as Supplementary Material for future reference; the present study is based on those data.

Although experimental studies on non-CARF accessory proteins have been limited to Cmr7 from *Sulfolobus* [13], numerous studies have investigated the role of common CARF family accessory proteins such as Csx1, Csm6 and Csa3. The crystal structure of Csa3 was first resolved in 2011 [14] and it demonstrated that the C-terminal DNA binding HTH domain was likely to be under allosteric control of the N-terminal Rossmann fold domain implicated in dinucleotide ligand sensing, of the type that is normally involved in signal recognition. Furthermore, a crystal structure of Cmr2, with its cyclase domain, was also compatible with the occurrence of such a signal [15]. These early insights were later undermined by genetic studies on Type III systems [16,17] that linked the presence of Csx1 and Csm6 to a DNA interference phenotype. This was enigmatic at the time because several crystallographic, biochemical and bioinformatic studies had predicted that the proteins must be primarily RNases [18–20]. A key proposal was subsequently made that Csx3 was a distant CARF family member and that the ligands sensed by CARF proteins in general were cyclic oligonucleotides [21,22]. This hypothesis was confirmed in three recent independent studies [23–25], two of which also showed that the cyclic oligoadenylate (cOA) signaling molecules were synthesized by the polymerase domain of Cas10 upon recognition of its target [15,26]. Apparently any target recognition by cellular Type III interference complexes triggers cOA synthesis which, in turn, ensures the coordinated activation of a potentially complex and layered defence response that is dependent on intracellular CARF proteins.

Although CARF proteins constitute the most widespread Type III accessory proteins, accessory proteins lacking CARF domains are much more diverse and almost as widespread. For example, it was shown that archaeal Type III interference gene cassettes are often flanked by diverse accessory genes encoding protein domains associated with nucleases, proteases, helicases, toxins or transcriptional regulators [1,13,16]. As for bacterial genomes, a search has already been undertaken specifically for CARF-encoding genes in both archaea and bacteria, and it yielded a comprehensive catalogue of CARF domain-carrying proteins [12]. Here we identify new families of non-CARF *cas* accessory genes associated with Type III modules, in addition to those encoding CARF domains, in archaeal and bacterial genomes. Since non-CARF accessory genes do

not share a common sequence motif or domain, they are particularly challenging to identify. Our method relies on a guilt-by-association approach, coupled with criteria for coevolution and specificity to exclude false positives. Type I, II, IV, V and VI *cas* gene cassettes were not examined systematically because the incidence of accessory genes is too low to distinguish signal from noise with our method given the limited number of annotated genomes available, although an independent study has been undertaken for these CRISPR-Cas types [27]. In the present study, by focusing on Type III systems, we are better able to identify reliable candidate accessory genes from a spurious gene background.

## 2. Results

From a total of 1263 archaeal and bacterial genomes in which CRISPR-Cas cassettes are fully annotated [2], 381 genomes encoded 512 distinct Type III genetic modules which were surveyed for accessory genes (Table 1). Selecting five genes immediately upstream and downstream from each module yielded a total of 4467 genes. This number was less than the theoretical total of 5120 genes because neighbouring adaptation modules, Type I interference modules and *cas6* genes were omitted from the analysis. All the encoded protein sequences were aligned with one another and a custom similarity metric [1] was calculated and used for Markov clustering (MCL) [28]. This yielded 231 gene clusters each with more than three members. Cas association scores were calculated for each gene cluster using information about Type III coevolution, Type III subtype specificity, and host genome self-similarity. Gene clusters with low Cas association scores were considered spurious and disregarded. The Cas association score ranged from 100 to –100 corresponding to a strong through weak Type III association, and a cut off of 24 was set by comparing the results to the manually curated accessory gene families obtained in the

**Table 1.** Summary of results from the current study compared to previous studies that identified accessory *cas* genes, divided between archaea and bacteria. The previous studies were limited to a (a) archaeal genomes [1] and (b) a representative subset of genomes [12]. The present study is more comprehensive.

	present study		Makarova 2014		Vestergaard 2014
	Ar	Ba	Ar	Ba	Ar
Number of genomes surveyed	217	2534	172	484	159
Number of genomes with CRISPR-Cas systems	131	1131	50	133	124
Number of genomes with Type III systems	78	304	34	114	83
Total number of Type III systems	110	402	61	251	125
Number of genomes with accessory genes	67	262	78	180	76
Total number of putative accessory genes	248	734	190	454	239
Accessory genes found outside <i>cas</i> cassettes	0	0	104	152	0
Accessory genes associated to Type III systems	248	734	61	251	210
Total number of non-CARF accessory genes found	136	369	0	0	135

previous archaeal genome study [1]. Thereafter, 76 of the 231 Type III-associated gene clusters were considered strongly associated; the remainder were discarded. The 76 gene clusters encompassed a total of 982 potential accessory genes distributed across the 512 Type III modules. This translated, on average, to two accessory genes per Type III module, varying from no additional genes to more than the core Type III genes (Figure 1). Properties of the 76 gene families are summarized (Table 2) and a more elaborate version (Table S1) is available online.

### 2.1. Online availability of results

The complete set of results is provided online in an indexed and readily searchable format for further validation (Table S1, <http://accessory.crispr.dk>). Multiple sequence alignments are provided for protein sequences encoded by each gene cluster. Gene names, and host genome accession numbers are given for each gene together with the adjacent Type III module subtype (Table S2, <http://accessory.crispr.dk/genes.html>). Profile-profile matches to the sequence family databases Pfam [29], TIGRFAMs [10] and CDD [11] are also presented for each gene family, along with matches to protein structures in PDB [30]. A multi-FASTA file containing all 982 accessory protein sequences along with the designated cluster ID is also available (<http://accessory.crispr.dk/Shah2018.TypeIIIaccessory.faa>). Finally, gene maps have been drawn for each of the 982 separate putative accessory genes found, illustrating their genomic context including the neighbouring Type III genetic module and other accessory genes or core *cas* genes from other systems flanking the same module. Clicking the gene maps links to the gene entry in the RefSeq database, enabling easy retrieval of protein or gene sequences, along with the option of initiating a BLAST or CDD search with an additional click. Code for reproducing the results is available GitHub (<https://github.com/BackofenLab/Accessory.Crispr>).

### 2.2. Largest gene clusters

Of the five largest gene clusters (1 to 5), the first three had 116, 94 and 69 members, respectively (Table 2). All gave highly significant profile-profile matches to known CARF protein profiles (e.g. TIGR02710 or Csx1 and the 5FSH PDB entry for the Csm6 crystal structure from *Thermus thermophilus*). This result confirms the earlier observation for archaea that CARF domain-encoding genes comprise the most dominant class of accessory genes. The largest cluster with no CARF match, cluster 4, had a low Cas association score (only 3% Type III specificity) and was considered spurious and not included in Table 2. This particular gene cluster encodes an ancient, ubiquitous, family of ABC-transporters with high sequence conservation that would probably appear enriched regardless of the genomic locus under survey. Gene cluster 5 with 64 members was almost exclusively associated with the less well characterised III-D subtype modules. These genes were always closely linked with their cognate Type III genetic modules and co-transcribed with the core *cas* genes. The genes encode a relatively small protein (about 160 aa) with no significant matches in sequence databases, a pattern typical for Cas11 (SS). Additionally, a *cas11* gene assignment for these systems was missing from the original 2015 annotation. Therefore, we inferred that the gene, like cluster 42 (Figure 1(e)), encodes the Cas11 analog, of an uncharacterized subfamily of Type III-D modules and that cluster 5 represents a core Type III-D gene family rather than an accessory gene family.

### 2.3. Most strongly associated gene clusters

The five most strongly associated accessory gene clusters according to the calculated Cas association score were clusters 83, 107, 108, 87 and 42 (Table 2). Cluster 83 carries six genes all located adjacent to Type III-A gene cassettes from cre-narchaeal orders including the thermoacidophilic Sulfolobales and the thermoneutrophilic Thermoproteales. These genes are invariably located immediately adjacent to cluster 17 genes

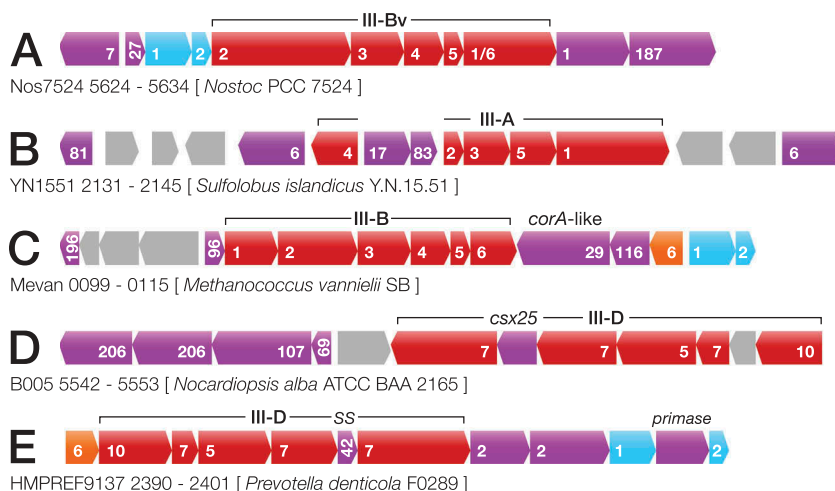


**Figure 1.** Gene maps of example Type III gene cassettes including accessory genes. Core Type III genes are drawn in red with *csm/cmr* numbers for Type III-A/B modules, and *cas* numbers for Type III-D modules. *cas6* and the adaptation module genes are orange and blue respectively, also with *cas* gene numbers. Accessory genes are drawn in purple with the gene cluster number indicated.

**Table 2.** List of putative accessory gene clusters conserved near Type III genetic modules which passed the Type III association score cut-off (>24). A few gene families with lower scores are also included because they have been confirmed as accessory proteins in earlier studies. For each putative accessory protein family, the cluster id, the size (i.e. number of members per cluster), and the calculated Type III association score are listed. An example (gene-) locus id is also provided for reference. Names are provided for accessory protein families identified in earlier studies [1,10,12], while those identified in the present study are indicated in bold with C3a numbers (Cas type 3 Associated). 39 of 76 putative accessory protein families are newly identified. Commonly associated Type III subtypes are listed for each putative accessory protein family. Unclassified variant subtypes are indicated by 'III'. Most accessory gene families can function with different Type III subtypes. A predicted function is given in the last column.

cluster	size	score	example	name	subtype	annotation
1	116	73.88	JTY_2831	Csx1/Csm6	A,B,D	CARF+HEPN
2	94	69.25	Selin_1039	Csx1	A,B,D	CARF+HEPN
3	69	62.33	FFONT_0074	Csm6	A,B,D	CARF+RelE
5	64	59.36	ERE_12150	Csx19/24	(A,B),D	core gene ( <i>cas11</i> )
6	61	58.51	TOPB45_1115	Csx1	A,B,(C,D)	CARF+HEPN
7	51	42.59	Tph_c24580	WYL/Csx1	A,B,D	CARF+WYL
9	49	37.91	Vdis_1148	Csx1	(A),B,(C,D)	CARF+Nuclease
11	41	35.59	Thebr_0941	Csx15/20	A,B,D	peptidase
17	31	24.7	VMUT_1481	Cas_RecF	A,B,(C,D)	SMC ATPase
23	20	4.61	CYB_0598	Csx1	(A),B,D	found elsewhere
25	18	55.83	Dtur_0613	Csx3	A,B,D	Csx3 (CARF)
27	17	50.07	Cyan10605_3521	Csx18	B,(D)	adaptation associated
28	17	66.76	CYB_0586	Csx21	17	Type III-D associated
29	14	45.91	CBO2177	CorA	B,(C),D	CorA-like
33	13	10.47	M1425_0883	Csa3	(A),B,C	Type I-A associated
35	12	61.07	CYB_0599	Csx3	(A),B,D	Csx3-AAA
36	11	50.71	Nos7107_4284	WYL	(A),B,D	HTH-WYL
37	11	56.62	SacN8_09300	Csx26	III,A,(B)	HNH nuclease
38	10	54.35	Mefer_0963	<b>C3a38</b>	A,B	unknown
42	9	74.4	CFT03427_1632	Csx19	D	core gene ( <i>cas11</i> )
43	9	58.83	Ferpe_1557	<b>C3a43</b>	A,B	Lon protease
45	9	28.54	Marme_0670	PD-DExK	A,B,D	possible nuclease
47	9	27.09	SacN8_09290	protease	III,A,B,D	peptidase
50	8	61.07	Swol_2530	Csx13	(A),B,D	TM+CARF
55	7	44.44	Nos7107_2836	<b>C3a55</b>	B,D	ABC permease
57	7	20.46	Calkr_2542	HerA	A,B,(C)	Type III coevolved
58	7	33.01	VMUT_1471	NurA	A,B	Type III coevolved
59	7	55.84	Nos7107_2826	<b>C3a59</b>	A,B,D	trans-membrane (TM)
64	7	43.07	SacRon12I_09300	<b>C3a64</b>	III,A	unknown
67	6	40.03	Caur_2269	<b>C3a67</b>	(A),B	AAA-Csx3
69	6	29.69	B005_5545	<b>C3a69</b>	D	unknown
76	6	39	LS215_0703	<b>C3a76</b>	III,A,D	unknown
77	6	29.73	NE0116	Csx16	A,B,D	a.k.a. cas_VVA1548
80	6	27.48	PTH_0706	<b>C3a80</b>	B,C,D	AAA+ ATPase
81	6	-9.48	YN1551_2131	Csx1	(A),B,D	Type I associated
83	6	88.69	VMUT_1493	cas_RFas	A,(B)	cluster 17 associated
84	6	66.57	TTX_1229	cas_RFas	A,(B)	cluster 17 associated
87	6	74.65	SSO1986	Cmr7	B	Cmr7
93	5	30.57	Thebr_0950	<b>C3a93</b>	B,C,D	poss. AAA ATPase
96	5	42.25	Mvol_0529	Mvol_0529-fam	B	DNA binding C-ter.
104	5	39.74	Msed_1167	Csx1	A,B,D	CARF+PIN
107	5	84.37	B005_5544	Csx1	B,D	CARF
108	5	78.8	Pcal_0278	cas_RFas	B	cluster 17 associated
116	4	57.92	Rru_A0181	<b>C3a116</b>	B,D	cluster 29 associated
121	4	62.04	Desac_1715	Csx23	A,B,D	unknown
123	4	37.09	Caur_2303	<b>C3a123</b>	B,D	unknown
124	4	44.42	PCC7418_1341	<b>C3a124</b>	B	unknown
139	4	28.91	Tthe_0931	<b>C3a139</b>	A,B,D	HKD+Snf2
146	4	68.43	SSO1421	<b>C3a146</b>	D	DNA binding HTH
152	3	25.85	Cylst_6373	<b>C3a152</b>	C	Type III-C specific
156	3	28.1	Metin_0159	<b>C3a156</b>	B,C	oxidoreductase
159	3	27.06	Calkr_2554	<b>C3a159</b>	A,B,C	methyl transferase
162	3	40.43	SYO3AOP1_0653	<b>C3a162</b>	III,A,B	unknown
166	3	32.1	Hbut_0719	<b>C3a166</b>	B,D	poss. crRNA proc.
168	3	31.1	slr7083	<b>C3a168</b>	B	unknown
173	3	70	Adeg_0988	Csx21	III,B,D	unknown
174	3	74.3	Adeg_0809	<b>C3a174</b>	B,C	nucleotidyl trans.
178	3	37.97	Csac_0071	<b>C3a178</b>	A,B,D	putative invertase
181	3	25.55	Tpen_1359	<b>C3a181</b>	A,B,C	Diadenylate cyclase
186	3	28.77	RoseRS_2594	<b>C3a186</b>	A,C,D	C-3',4' desaturase
187	3	39	Dole_0738	<b>C3a187</b>	A,B	NERD+UvrD
189	3	50.73	Hoch_5581	<b>C3a189</b>	B,D	kinase
193	3	43.78	Thebr_0949	<b>C3a193</b>	B,D	poss. alt. Cas3
194	3	26.83	Mcup_1132	<b>C3a194</b>	B,D	AA transporter
196	3	46.29	TREPR_1099	<b>C3a196</b>	III,A,B	unknown
198	3	40.67	Mrub_1490	<b>C3a198</b>	B	TPR protein
205	3	67.5	MLP_11360	<b>C3a205</b>	D	unknown
206	3	29.39	Ndas_2980	<b>C3a206</b>	D	TAP-like protein
211	3	51.67	Pars_1112	cas_RFas	B	unknown
212	3	39.67	RoseRS_0371	<b>C3a212</b>	C,D	SNc+LTD
214	3	30.16	Rcas_4246	<b>C3a214</b>	B,C	GlgB
216	3	25.6	SSA_1254	<b>C3a216</b>	A,B	adaptation associated
222	3	44	Vpar_1800	<b>C3a222</b>	A,D	unknown
223	3	43.33	YG5714_0635	<b>C3a223</b>	III,D	unknown
227	3	36.73	Sfum_1354	PrimPol	A,B	adaptation polymerase
230	3	28.76	TVNIR_1454	<b>C3a230</b>	B	RecX family protein



(Figure 1(b)) encoding a putative ATPase domain protein (330 aa) (Table 2) common to DNA repair proteins of the SMC (Structural Maintenance of Chromosomes) type including rad50 and recF. The protein sequences that make up cluster 83 average 160 aa and yield no good profile matches in public databases. The cluster 83–17 pair of accessory genes is also accompanied by gene clusters 6 and 84 (Figure 1(b)), the former of which encodes a CARF protein of the MJ1666 type [10], while genes of the latter are similar in size to those of cluster 83 and appear to show weak sequence similarity.

Cluster 107 has five gene members present in divergent bacterial genera *Nocardiopsis* and *Thermus*, members of the *Actinobacterial* and *Thermus-Deinococcus* phyla, respectively. Cluster 107 proteins produce significant sequence matches to known CARF domain-containing proteins but are larger (about 700 aa) and long regions in the middle and at the C-terminal end yield no profile-profile matches in databases. Thus, while it is likely that these CARF proteins are also activated by cOA, their effector function remains obscure. In *Nocardiopsis* the host carries subtype III-D modules (Figure 1(d)) and also harbours cluster 206 genes which encode a protease of the AB hydrolase family. Typically for CARF proteins, cluster 107 is found associated with different subtypes III-B and III-D.

Cluster 108 genes are found amongst crenarchaeal thermo-neutrophiles, often in multiple divergent copies immediately adjacent to cluster 17 genes, similar to the coexistence of genes of clusters 17, 83 and 84. Cluster 108 proteins (about 180 aa) show no sequence similarity to cluster 83/84 proteins and yield no good matches to protein family databases. However, they contain a transmembrane (TM) signal at the N-terminal end consistent with the protein being membrane bound.

Cluster 87 corresponds to *cmr7* [13] and is an additional *cas* gene so far exclusive to *Sulfolobus* species. Exceptionally Cmr7 has been characterized experimentally and shown to associate tightly with the Cas10/Cmr3 sub-complex within the cognate Type III-B effector complex [13]. Cluster 87 genes are associated exclusively with the Cmr- $\beta$  subclass of *Sulfolobus* Type III-B modules. Cmr- $\beta$  exhibits RNase activity cleaving at U-A dinucleotide pairs [13] whereas most other Type III-B complexes cleave at regular spatial intervals along the target RNA, via their Cmr4 subunit [31–33].

Cluster 42, like cluster 5, contains an uncharacterized Type III-D core gene encoding the Cas11 small subunit (SS) analog of a subclass of Type III systems which, to date, are poorly characterized. The genes are always located within the Type III-D gene cassette and appear co-transcribed with the other Type III-D interference genes (Figure 1(e)). The subclass of Type III-D modules carrying the gene cluster occur in the bacterial species *Campylobacter*, *Helicobacter*, *Fibrobacter*, *Tannerella* and *Saprosira*.

#### 2.4. Least strongly associated gene clusters

Some gene families were enriched adjacent to Type III genetic modules but were predicted not to be cofunctional. The ten lowest ranking Type III-associated gene families according to the Cas association score are summarized (Table 3). They are dominated by different transposase domains, and include a single ABC transporter family, all of which are ubiquitous in the mobilome

**Table 3.** The ten lowest ranking genes in terms of significance of association to Type III modules, based on the Type III association score. Even though these gene clusters are often found near genomic Type III systems, they are inferred not to bear any functional link with them, and, therefore, were not considered accessory.

cluster	size	score	example locus	domain matches	comments
209	3	-88.9	CFBS_2969	InsA	putative transposase
82	6	-72.2	UDA_2812	rve/Tra5	integrase/transposase
144	4	-66.3	Pcal_0278	COG5552/DUF2277	unknown function
12	39	-60.4	SSO1518	Trp 1/InsE	transposase
54	8	-46.7	MAF_28180	Int C/XerC	tyrosine recombinase
48	9	-42.6	YN1551_2375	InsG/IS 4	transposase
169	3	-33.3	Cagg_3808	Ftn	nonheme ferritin
8	51	-33.0	Smar_0302	PotA/MalK	ABC transporter
153	3	-32.6	Athe_0143	AmyAc MTase	alpha amylase
154	3	-30.33	Athe_0142	Yqil	trans-membrane

and, therefore, less significant. The result reinforces that Type III genetic modules tend to lie in genomic regions with relatively high HGT activity. The result also underlines the importance of employing criteria for coevolution and specificity, in addition to conservation, when searching for *cas* accessory genes.

#### 2.5. Diversity of accessory proteins with no CARF domain

Although CARF proteins are the most common accessory proteins, their diversity is quite limited with the CARF domain linked to different combinations of a few domains including HTH, WYL, HEPN and PIN toxins. In contrast, the non-CARF accessory proteins appear more diverse, exhibiting a wider range of protein domains and their genes span many smaller gene clusters. Nevertheless, some domain classes are more common than others and they are covered below.

Nucleases constitute the broadest class of non-CARF accessory proteins, associated with clusters 37, 45, 58, 139, 166, 187 and 212. Clusters 37 and 45 encode unrelated restriction endonuclease domains and cluster 37 is probably a core *cas* gene family for the *Sulfolobus* subtype III<sub>V-1</sub> system, judging from observed gene synteny. The protein may associate with the Type III effector complex, and facilitate DNA targeting. Cluster 45 genes may encode restriction activity against invader DNA and complement Type III DNA targeting activity. Cluster 166 proteins give good matches to the Nob1 rRNA maturation endonuclease and may be involved in crRNA maturation given that the associated Type III modules are not linked to a *cas6* gene. Nucleases encoded by clusters 58, 139 and 187 are all associated with helicase domains, either as a separate domain in the protein or encoded by co-transcribed genes. Type III systems lack the processive invader dsDNA digestion characteristic of Type I systems, via Cas3, and helicase/nuclease combinations such as the above may contribute the same type of functionality to Type III systems.

Proteases and peptidases represent an important class of non-CARF accessory proteins encoded by clusters 11, 43, 47 and 206. Clusters 43 and 206 encode relatively long proteins possibly with multiple domains that remain of unknown function. Clusters 11 and 47 encode small single domain proteins (about 100 aa), most of which match aspartic acid

peptidases. Some cluster 11 members carry no identifiable domains, reminiscent of core Cas11 proteins and may have co-clustered with the peptidases as a result of sequence similarity cut-offs being set too low. However, genes encoding viable peptidases are often found within operons of the cognate Type III Cas proteins which suggests that they are core effector genes and may be involved in maturation of Cas proteins.

ABC and AAA ATPases comprise another well represented group of putative non-CARF accessory proteins with the cluster 17-encoded SMC ATPase being the most prominent (Figure 1(b)). Clusters 80 and 93 also encode ATPase domains. The former produces a large protein matching DUF499 in Pfam that probably contains multiple domains and resembles SMC and RecF ATPases at the C terminal end. Cluster 93 encodes a small protein and often accompanies cluster 80, with their genes sometimes co-transcribed, and they carry an AAA ATPase motif. Cluster 35 encodes a protein family found mainly in cyanobacteria; it has a Csx3 domain in the N-terminal end and an AAA ATPase domain in the C-terminal region. Cluster 67 is similar but encodes the domains organized in the opposite order. Csx3 is predicted to be a distant member of the CARF superfamily [22], and the AAA ATPase is likely to be under allosteric regulation from the CARF domain, with a cOA signal as possible activator.

Another class of accessory gene families are linked to Type III adaptation modules. Members are often located adjacent to adaptation genes including *cas1* and *cas2*. Cluster 227 encodes a primase domain and is found with adaptation modules of Type III-A and Type III-B systems. A related gene occurs adjacent to Type III-D-linked adaptation modules (Figure 1(e)). Functions may include DNA repair following spacer acquisition, or a replacement for Cas4, or reverse transcription to generate DNA spacers from RNA invaders. The cyanobacterial Type III-B associated clusters 216 and 27 (Figure 1(a)) encode small proteins and the former matches a part of Cas1 from Type III-A-associated adaptation modules of other bacteria. Since Type III interference is protospacer adjacent motif (PAM)-independent, this Cas1-associated domain may have evolved to bypass the requirement for a spacer acquisition motif (SAM) [34] that occurs in Type I and II systems.

A final class of putative accessory gene families includes those encoding proteins with no significant domain matches. Most of them are small (100 to 200 aa) but a few are larger including those of cluster 124 (average 430 aa). Gene families without identifiable encoded domains are sometimes associated with other accessory genes, including the Cas\_RecF-associated gene families (clusters 83, 84 and 108) (Figure 1(b)) [1], the CorA-associated cluster 96 (Figure 1(c)) and cluster 38 which is often associated with cluster 43-encoded

proteases. Other clusters occur alone (cluster 76) or show no clear association pattern (cluster 69), indicating that they can function independently from other accessory proteins.

Next we present two experimental sections to gain further insights into the potential roles and significance of a few accessory proteins. The first constitutes a study of the cyanobacterium *Synechocystis* sp. PCC 6803 where a series of accessory genes was selectively deleted and the effect on Type III-B interference and crRNA maturation was investigated. In the second, the dependence of RNase activity on cyclic adenylates was examined for accessory proteins of Type III-B systems of *Sulfolobus* with a view to compare the results with those obtained earlier on bacterial Type III-A systems.

## 2.6. Type III-B interference activity was not directly impaired in candidate accessory gene deletion mutants

The major defense plasmid pSYSYA, present in the cyanobacterium *Synechocystis* sp. PCC 6803, harbours three separate CRISPR-Cas systems – CRISPR1, CRISPR2 and CRISPR3. CRISPR1 and 2 are classified as subtype I-D and III-D CRISPR-Cas systems, respectively [35–37], while CRISPR3 is a subtype III-B variant system (III-Bv) carrying an unusual fusion of Cmr1-Cmr6 and lacks an obvious Cas6 homolog<sup>38</sup>, (Figure 2). Recently, it was demonstrated that CRISPR3 is a viable CRISPR-Cas system that functions independently of the non-cognate Cas6 endonucleases associated with CRISPR1 and CRISPR2. In addition, the host-encoded RNase E was shown to perform crRNA processing in *Synechocystis* sp. PCC 6803 [38].

To test the functionality of the CRISPR3 system in wild type *Synechocystis* sp. PCC 6803, an interference assay was developed based on two invader plasmids, each containing the reporter gene gentamicin and a fused protospacer sequence in either sense or antisense orientation [38]. In this study, the same assay was used to test the effects of single candidate accessory gene knock-outs on interference activity. For each accessory gene knock-out mutant we observed a significant reduction in the number of transconjugants for both invader plasmids relative to the control (Figure 3(a)), as previously seen for wild type *Synechocystis* sp. PCC 6803 [38]. Hence, the interference system was fully operational. We conclude that the gene products of the investigated accessory genes are not directly involved in the interference stage as the efficient degradation of invading nucleic acids was not impaired in any tested mutant strain and behaved the same as the wild type strain. However, we found that the abundance of CRISPR3 crRNA transcripts was clearly reduced in the knock-out strain of the accessory gene *slr7088* (Figure 3(b)) belonging to cluster 11 and encoding a peptidase within the



**Figure 2.** Gene map of the *Synechocystis* sp. PCC 6803 pSYSYA Type III-Bv module with flanking genes. Core Type III genes are coloured red and denoted with Cmr numbers. Adaptation module genes are coloured blue and marked with Cas protein numbers. Accessory genes found in this study are coloured purple and indicated with cluster numbers. Genes deleted in mutants subject to the interference assay are marked by a dot below. None of the individual deletions resulted in a marked decrease in interference activity.

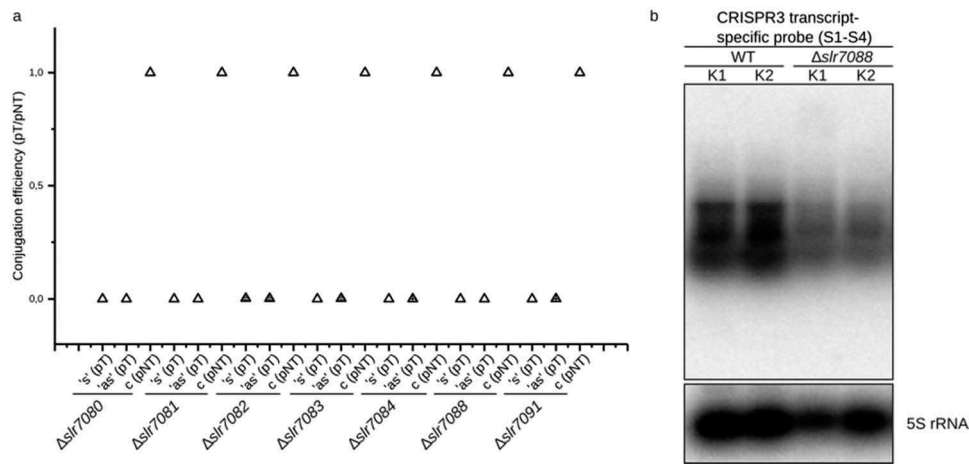


**Figure 3.** Experimental investigation of accessory gene knock-out mutants in *Synechocystis* sp. PCC 6803. a) Interference activity of subtype III-Bv-associated accessory gene knock-out mutants. Conjugation efficiencies are calculated by the ratio of the plasmid target (pT) to the plasmid non-target (pNT, control). The conjugation efficiency of the control plasmid was set to 1 and the number of colonies for the plasmid targets was normalized to the control plasmid. Data points represent mean values and standard deviations were calculated for three independent biological replicates. The accessory gene *slr7080* is included in cluster 35, *slr7083* in cluster 168 and *slr7088* belongs to cluster 11. 's', invader plasmid with protospacer in sense orientation, 'as', in antisense orientation, 'c', control plasmid without protospacer. b) Northern hybridization using a radioactively labelled transcript probe spanning CRISPR3 spacers 1–4. The knock-out mutant *Δslr7088* shows decreased CRISPR3 crRNA accumulation compared to the wildtype (WT) strain. After normalization against 5S rRNA the WT clones accumulated in average 1.24 times more CRISPR3 crRNA than the *slr7088* deletion mutants. A representative of two independent experiments is shown.

CRISPR3 Cas cassette [38]. Therefore, the selected accessory genes do not appear to encode any functionality with regard to the interference stage but they might well play a role in other CRISPR-Cas related processes, e.g. affecting CRISPR3 crRNA stability and/or turnover as demonstrated for *slr7088*.

## 2.7. Compatibility between SisCmr- $\alpha$ and different *Sulfolobus* CARF proteins

Most putative accessory gene families, especially those encoding CARF proteins, can associate with different Type III subtypes (Table 2). Moreover, highly similar CARF genes, including *sisCsx1* (locus tag: SiRe\_0884) are also located adjacent to gene cassettes of different Type III subtypes (Figure 4). This suggests that some degree of compatibility can occur between CARF proteins and different Type III subtypes.

The Type III-B system (Cmr- $\alpha$ ) of *Sulfolobus islandicus* (Sis) synthesizes cyclic tetra-adenylate (c-A4) which binds to the CARF domain of SisCsx1, the cognate accessory RNase of Cmr- $\alpha$ , producing strong RNase activity (WH, QS unpublished). We examined the potential for c-A4 to activate three additional *Sulfolobus* CARF proteins, namely SiRe\_0765 (Csa3), SiRe\_0811 (Csm6) and ST0035 (a CARF-PIN toxin) from *S. tokodaii*. ST0035 was shown, by UV crosslinking, to weakly interact with c-A4 but it did not induce additional

RNase activity. SisCsx1 was the only protein that interacted strongly with c-A4, leading to efficient induction of RNA cleavage by activation of the HEPN toxin domain. It was concluded that the other *Sulfolobus* CARF proteins may be activated by other species of cOAs synthesized by different Type III effector systems within the cells.

Although the comparative genomics results suggest that compatibility can occur between CARF proteins and different Type III subtypes, the experiment indicates that this is not a general rule and that other factors may be important for the CARF protein-Type III association to be productive.

## 3. Discussion

The computational method developed for identifying putative accessory genes employed similarity cut-offs and criteria for defining clusters based on considerable prior experience with manual annotation of genomic CRISPR-Cas cassettes. The Type III association score, based on criteria for host genome self-similarity, Type III specificity and coevolution, yields good granular control over sensitivity versus specificity. The cut-off employed involves a tradeoff which produced a few false positives and some false negatives. However, we infer that the vast majority of the gene clusters selected do carry some level of Type III accessory functionality (Table 2). The

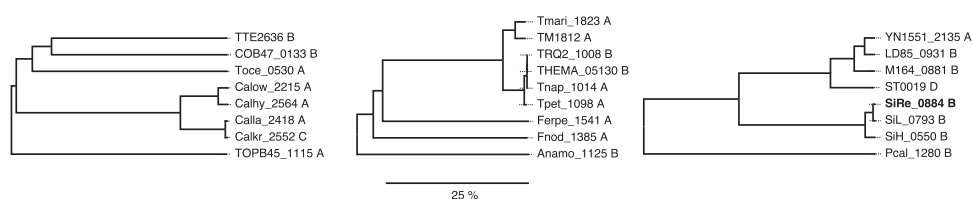


**Figure 4.** Three subtrees from a neighbor-joining tree of all CARF proteins found in this study. Gene (locus) ids are shown along with the subtype of the associated Type III system. The branch length corresponding to a 25% dissimilarity at the amino acid sequence level is indicated with the ruler. Closely similar CARF proteins can associate with, and cofunction with, different subtypes of Type III systems. SisCsx1 is included in the final subtree (in bold).

method relies on accurate prior annotation of Type III core genes so that flanking genes can be evaluated; for inaccurately annotated Type III systems the method may identify core *cas* genes as accessory genes.

The fact that the most widespread CARF and non-CARF accessory genes were identified previously (Table 2) does not undermine the significance of our approach. Accessory protein families have been defined and annotated over a decade involving extensive manual comparisons and curation whereas the present method is semi automatic and scalable and can accelerate the discovery of non-CARF accessory proteins, especially when coupled to an automated pipeline for annotating CRISPR-Cas systems in newly sequenced genomes, an approach that is being developed [2]. The present study indicates that the diversity of non-CARF accessory proteins is still under-sampled whereas the major families of CARF accessory proteins have probably been identified [12]. Searching additional diverse genomes, and metagenomes with the method, should help identify new accessory protein families with increased precision. Therefore, we plan to integrate the current method into our earlier methods [1,2,39–41] and generate a fully automated system for annotation and characterisation of CRISPR-Cas systems.

### 3.1. Detection of previously confirmed accessory proteins

37 of the 76 accessory gene families have been noted in previous comparative genome studies (Table 2). The most important group comprise CARF proteins that were characterized at an early stage [10] and were more recently catalogued systematically together with WYL domain proteins [12]. The major families of previously characterized accessory proteins lacking CARF domains include: (a) clusters 5 and 42 (C<sub>sx19</sub> and 24) that are annotated as CRISPR-associated in the TIGRFAMs database, and are both likely to encode core Type III Cas11 proteins; (b) clusters 57 and 58 encode the HerA/NurA helicase-nuclease pair and were initially found associated with crenarchaeal thermoneutrophile Type III systems [42] and later found in other crenarchaea and eukaryotes [1]; (c) cluster 29 encodes a CorA-like putative magnesium transporter and was originally found linked to Type III-B systems in *Methanococcus* and *Clostridium* [1]; here we show it also occurs adjacent to Type III-D systems and in diverse bacteria; (d) cluster 11 or *csx15/20* encodes a Type III-associated peptidase that is erroneously catalogued in CDD as being Type I-U associated [11]; we found here that it is linked to crRNA biogenesis in *Synechocystis*; (e) cluster 47 encodes a Type III-associated peptidase found together with cluster 37 encoding a nuclease; both are associated with the crenarchaeal III<sub>V-1</sub> variant subtype [1] and may comprise core *cas* genes for this Type III subtype; (f) cluster 17 or Cas\_RecF encodes a repair-associated ABC ATPase found adjacent to diverse crenarchaeal Type III genetic modules [1] and it is often accompanied by clusters 83, 84 and 108 which do not yield significant sequence database matches. ATPases, although common and functionally diverse, are well conserved sequence-wise and while a functional link to

DNA repair is possible it could be an artefact. However, ATPases could provide the energy required for shifting the chemical equilibrium towards more efficient cleavage of target nucleic acid, given that Type III systems lack the helicases of Type I systems that ensure processive target cleavage.

During the review process of this manuscript, another manuscript was released in preprint [27] which also describes the detection of new *cas* genes. The authors used a similar approach by employing a score, but looked at genes flanking all Cas types in addition to CRISPR arrays. In spite of having used twice the number of input genomes they only found around half the number of accessory proteins found here (560 proteins covering 58 profiles). The lower sensitivity may have resulted from the noise coming from a broader search. Data from both studies should prove valuable for future experimental validation, due to their respective deep vs. wide approaches yielding independent results.

### 3.2. Compatibility between CARF accessory proteins and different type III subtypes

The results (Table 2, Figure 4) suggest that CARF accessory proteins in particular are able to cofunction with various Type III systems regardless of subtype. A mechanistic rationale for this compatibility could be the shared capacity of Type III subtypes to synthesize the cOA signal required to activate CARF proteins upon invader RNA recognition. The CARF domain is likely invariant for Type III modules as long as a cOA messenger can activate it. While this explains the observed subtype compatibility, experimental evidence from Type III-A systems in *Streptococcus thermophilus* (St), *Thermus thermophilus* (Tt) and *Enterococcus italicus* (Ei) [23,24] and a Type III-B system in *Sulfolobus islandicus* (Sis) (WH, QS unpublished), suggest that the mechanisms are more complex (Table 4). The different Type III-A Csm effector complexes tested produced different cOA profiles; some synthesising mostly cyclic hexa-adenylate (c-A6) while others produced mainly cyclic triadenylate (c-A3). The archaeal Type III-B system synthesized a signal dominated by cyclic tetra-adenylate (c-A4) (WH, QS unpublished). Moreover, the synthesis efficiencies varied by more than an order of magnitude between the different Csm and Cmr effector complexes tested (Table 4) and the *E. italicus* system had to be genetically modified to produce significant yields. In addition, the CARF RNases tested showed strong preferences for specific cOA species, with some favouring c-A6 and others c-A4 and, moreover, their activation efficiencies varied markedly, with some CARF proteins requiring several orders of magnitude higher cOA concentrations to trigger efficient RNA digestion.

The cOA specificities of CARF proteins and the effector complexes appear to transcend the broad protein family, and effector subtype categories, because they presumably vary over shorter evolutionary distances. For example, the Type III subtypes are not linked to specific cOA species (Table 4) and such mechanistic differences probably occur at a finer subfamily level.

CARF accessory proteins and core Type III effectors must be able to cofunction in order for their linked genes to persist.



**Table 4.** Comparisons of reaction efficiencies of different CARF proteins with respect to RNase activity, and for Type III effector complexes with respect to cOA synthesis. Substrates comprise RNA for CARF proteins and ATP for Type III complexes. Reaction times, substrate and effector concentrations shown are the minimum required for digestion of 50% of the RNA substrate or for converting more than 80% of ATP into cOA. The concentration of cOA required for activation of CARF proteins differs by several orders of magnitude, as does the efficiency with which the Type III complexes synthesize cOA. The c-A6 required to activate StCsm's cognate Csm6 protein comprises a minor species (only 0.5% total cOA synthesized), with the major species being c-A3. In contrast, almost all cOA synthesized by SisCmr and EiCsm\* was of the type required by cognate CARF proteins. Table contents were compiled from published data [23,24]. EiCsm\* contained dEiCsm3, a nuclease-dead mutant protein. The SisCsx1 and SisCmr data were produced in the Copenhagen laboratory (WH, QS unpublished).

	SisCsx1	TtCsm6	StCsm6	StCsm6'	EiCsm6	SisCmr	StCsm	EiCsm*
class	Csx1	Csm6	Csm6	Csm6	Csm6	III-B	III-A	III-A
active cOA species	c-A4	c-A4	c-A6	c-A6	c-A6	c-A4	c-A6	c-A6
effector conc (nM)	100	10	0.1	1	0.15	10	200	160
Substrate	520 nM	10 nM	10 nM	10 nM	40 nM	100 μM	50 μM	500 μM
cOA (nM)	20	500	0.5	5	5	~ 70%	0.5 %	~ 100 %
reaction time (min)	20	30	30	30	4	20	10	30

However, the experiments summarized above indicate that variables such as the sensitivity to the signal, the species and its concentration, limit productive CARF-Type III interactions.

### 3.3. Mobilome-associated genes adjacent to type III modules

In addition to accessory gene families, we expected mobilome-associated gene families to be enriched around genomic Type III *cas* modules. The Type III association score was devised to address this problem, and five out of the ten lowest ranking gene clusters encoded putative transposases (Table 3). Remarkably, no toxin-antitoxin (TA) gene pairs were found despite (a) previous studies showing that they are common in mobilomes, with some bordering CRISPR-Cas modules [43,44] and (b) additional evidence demonstrating coevolution between TA gene pairs and adjacent Type III modules [45]. The TA systems may influence mobility of adjacent CRISPR-Cas modules or they may help induce dormancy or programmed cell death at key stages of the immune response, in order to minimize the spread of invader genetic material in the cellular population [18]. Thus, they could provide a semi-accessory function to Type III immunity while also being able to function independently. This would explain why some specific subfamilies of TA systems are enriched adjacent to CRISPR-Cas gene cassettes while others are not [45] and, as a result, they were not detected by our method.

Of the many accessory proteins identified that yield no protein domain matches with databases some of these could be anti-anti-CRISPR proteins. An increasing number of anti-CRISPR proteins have been characterized, encoded by phages [46] and by archaeal viruses [47], and it remains a possibility that some of the CRISPR-Cas systems encode accessory proteins that can neutralize the anti-CRISPR proteins before they inhibit an immune response.

### 3.4. On the role of Type I associated CARF proteins

Type III effectors activate CARF proteins via a cOA messenger molecule signaling the presence of intracellular invader RNA [23–25] and many CARF protein genes were identified earlier adjacent to Type III modules [10,48]. Less clear is why CARF protein genes are common adjacent to Type I systems,

especially amongst archaeal hyperthermophiles [1], when Type I core Cas proteins do not apparently possess the GGDD domain responsible for cOA derivatives. Most types of CARF protein genes that are associated with Type III modules, are occasionally found adjacent to Type I cassettes, with *csx3* and especially *csa3* being the most common. *csa3* encodes a transcriptional repressor of Type I-A interference modules with a DNA binding HTH domain coupled to a ligand sensing CARF domain. Its pattern of invariant presence suggests that it is a core gene for that subtype.

Type I-A gene cassettes in several *crenarchaeal thermoacidophiles*, including species of *Sulfolobus*, *Thermosphaera*, *Thermogladius*, *Fervidicoccus* and *Desulfurococcus* carry two *csa3* genes and recent studies have shown that one encodes a transcriptional repressor of Type I interference [49] while the other activates the adaptation module [50]. The former study detected invader nucleic acid-dependent activation of transcription of the Type I-A interference gene cassette. Moreover, a model was proposed that involved Csa3 binding to the Type I-A effector complex which then bound to the interference module promoter and repressed further transcription. Protospacer-containing DNA then recruited the effector complex and derepressed the Type I-A interference operon. A more likely model, given our current knowledge of Type III systems, involves sensing of invader nucleic acid by a Type III effector complex and, after recognition of invader RNA, the cOA signal produced may derepress the Type I-A interference module by inducing a conformational change in its CARF domain-containing transcriptional repressor. This model would also imply that spacer acquisition is under the positive control of Type III-mediated invader sensing, reminiscent of the primed adaptation seen for other Type I subtypes but involving a different mechanism. Thus, all CARF proteins associated with Type I systems may facilitate cofunctioning with Type III systems, either directly, as for Csa3, or indirectly by selecting for two types of CRISPR-Cas systems. Genomes that harbour Type I systems flanked by CARF genes like *csx1* are thus more likely to exhibit and maintain Type III systems, even when located on a distant genomic locus. This model also implies that Type I-A systems can be dependent on Type III systems for activating spacer acquisition and/or effector functions. Such an interdependence could give rise to synergies that would ensure a more robust immune response

in a natural environment with extensive viral diversity, especially as occurs amongst archaeal hyperthermophiles.

### 3.5. Type III systems as a general purpose RNA interference platform

Our finding that deletion mutants of *Synechocystis* sp. PCC 6803 Type III-Bv accessory gene candidates were not impaired in interference activity confirmed that RNA silencing and transcription-dependent DNA silencing are inherent to core Type III functionality and do not rely on accessory gene functions. The additional functions provided by the deleted accessory genes are likely to lie beyond basic interference. Furthermore, it was shown that the gene product of one accessory candidate gene, *slr7088*, is involved in crRNA stability and/or turnover, further supporting an auxiliary rather than a core role.

The extensive diversity of non-CARF accessory gene families located adjacent to Type III interference modules, suggests that they are multifunctional, likely extending functionality beyond immune defence. The basic RNA interference activity of core Type III effectors is non-processive in contrast to Type I interference activity where Cas3 processively digests invader DNA after protospacer recognition [51–53]. Type I systems are streamlined towards efficient invader dsDNA degradation, whereas core Type III systems are more versatile interfering with different types and configurations of nucleic acid. Thus Type III systems may be more useful for invader surveillance than clearance, and the cOA signaling pathway is ideal for directing effector functionality to other cellular systems. The specialisation of Type I systems towards supercoiled dsDNA targets suggests that they could have evolved from a more general purpose Type III-like ancestor, after the addition of a helicase-nuclease pair. This is also consistent with a recent hypothesis for evolution of Type I systems from Type III systems [54]. Adaptive immunity, although important, could well be one specialisation from a pool of functions offered by Type III systems. RNA interference has a variety of potential applications beyond immunity, particularly within information processing, and different accessory proteins may provide the crucial functional links to other cellular systems.

## 4. Concluding remarks

The developed computational method successfully identified 76 putative accessory gene families flanking genomic Type III genetic modules of archaea and bacteria, more than half of which had not been identified previously. The results expand in particular the repertoire of diverse non-CARF accessory gene families for which functions are currently unknown. One of the detected accessory protein families was found to be involved crRNA biogenesis efficiency for a Type III-Bv system in *Synechocystis*. The diversity of the gene families found provides evidence of Type III systems being coupled to numerous functions additional to invader nucleic acid silencing. The study also suggests that more accessory gene families will be detected in the future when

automated annotation of an increasing number of genomic CRISPR-Cas cassettes becomes available.

## 5. Materials and methods

The comparative genomics method for detecting putative accessory genes employs a ‘guilt-by-association’ approach, where genes flanking known Type III modules are first clustered by sequence similarity. The extent of conservation across a wide range of host genomes is taken as an indication that the flanking gene clusters are functionally linked to their cognate Type III modules. Since genomic CRISPR-Cas cassettes are most often located in genomic regions implicated in regular horizontal gene transfer (HGT), the mobilome, any genes flanking the cassettes will be shuffled even over short evolutionary distances. The method assumes that gene conservation adjoining Type III gene modules over larger evolutionary distances stems from a selective pressure to maintain those genes in close vicinity of the cognate Type III systems, indicative of a likely functional link. The mechanistic rationale underlying this, is that any horizontal transfer event involving a Type III module will be more likely to include any co-functional accessory genes the closer they are located to the core genetic module. This would ensure the transfer of fully functional cassettes into a new host and provide it with a selective advantage, and increase the chances of the cassette replicating in the new host.

The method used for identifying putative accessory genes relies on prior accurate annotation of core Type III genes. Therefore, the data set of annotated Type III modules from the latest CRISPR-Cas classification update is used [2]. For less well annotated Type III modules, the method is expected to pick up core genes in addition to any accessory genes. Furthermore, some gene families with no functional link may border Type III genetic modules and be enriched. Such gene families may include transposases, toxin-antitoxin gene pairs and genes within mobile genetic elements, all of which are generally enriched in mobilome regions. To distinguish true accessory genes from such false positive gene clusters, the Type III specificity and degree of Type III coevolution is estimated for each gene cluster. Gene clusters that have a history of accompanying Type III systems are predicted to display a high degree of coevolution and specificity for their cognate Type III module, and the results can thus be used to remove spurious gene clusters from those that are functionally conserved. By setting optimal cutoffs for defining gene clusters, specificities and estimates for coevolution, it is expected that most genes that pass them comprise accessory genes. While false positives may still occur, the chances of them being selected is minimized.

### 5.1. Definition of putative accessory gene clusters

Five genes upstream and downstream of annotated Type III gene modules were selected from the most recently classified archaeal and bacterial CRISPR-Cas systems [2]. They were then pooled and subjected to an all-against-all protein sequence similarity comparison. Alignments with an E-value above 1 were discarded as were alignments shorter than 40%

of the length of each of the two proteins in question. A further filtering step that took into account total protein sizes in relation to alignment length and the relative locations of similar sequence regions between the two compared proteins was performed to detect orthologous pairs of proteins (Equation 1).

$$\left| \frac{l_i}{l_j} - 1 \right| - \left( \sqrt[4]{\frac{e_i - b_i}{2 \cdot l_i} + \frac{e_j - b_j}{2 \cdot l_j}} - 0.8 \right) + \left| \frac{(b_i + e_i) - (b_j + e_j)}{l_i + l_j} \right| \leq 0.1$$

**Equation 1:** For the two compared proteins  $i$  and  $j$ ,  $l$  denotes their respective lengths,  $b$  the position of the beginning of the alignment and  $e$  the end. The sum of the three addends must not exceed 0.1 for the proteins to be considered orthologs. The size disparity and alignment positioning disparity (first and last addends) are thus penalized against the compensating (transformed) alignment coverage (middle addend).

Protein pairs which passed the filter were considered orthologous and forwarded to Markov clustering [28] which generated the clusters of orthologous proteins. A multiple sequence alignment (MSA) was made for each gene cluster using MUSCLE [55] and used for sensitive profile-profile sequence searches [56] against the PFAM, CDD, TIGRFAMS and COG databases [10,11,26,29] as well as the latest version of the PDB70 database that is distributed together with the HHSuite package [30,56]. The database searches were used to make rudimentary predictions of protein function (Table 2 and S1). MSAs were initially also used for a phylogenetic analyses in order to clarify whether the gene clusters had co-evolved with their cognate Type III systems. Aggregating scores from multiple pairwise alignments was introduced later to automate this step in order to estimate Type III co-evolution (Equation 2). Subclusters were defined for each cluster in order to estimate diversity and as a fall-back option when the main clusters were too broad. Hidden Markov models (HMMs) corresponding to each cluster were constructed and used for genome-wide searches to quantify the specificity of each gene cluster with regard to Type III gene module association. Later, pairwise sequence similarity searches were used for this purpose, as the results proved more accurate. A cas association score was then devised to distinguish spuriously associated gene families from those that were strongly associated. The score combined a coevolution and Type III specificity estimate, along with an estimate for the self-similarity of hosts carrying the gene cluster according to Equation 2.

$$\left( \frac{\sum_{i=1}^c \sum_{i=1}^c o_i}{c^2} - \frac{\sum_{j=2}^c \sum_{i=1}^c \frac{s_{ij}}{s_{ii}}}{c(c-1)} \right) \cdot 100 \leq 24$$

**Equation 2:** Let  $c$  be an integer denoting the size of the cluster of interest,  $i$  the  $i^{\text{th}}$  member of the cluster, and  $o$  a logical vector of length  $c$  with boolean values for whether the top  $c$  best genome wide orthologs (according to Equation 1) were already flanking Type III systems. Summing the contents of that vector and dividing it by  $c$ , and obtaining the mean of

that quantity for all members of the cluster yields the average proportion of cluster orthologs that are Type III adjacent. This quantity (i.e. the first addend) denotes the cluster Type III specificity and also comprises a measure for co-evolution, because only the best matching  $c$  orthologs are considered as opposed to all found orthologs that may include recently diverged paralogs. The other addend represents the cluster self similarity (taken as an estimate for host self similarity), which is the alignment score  $s$  of each member protein against another member protein  $j$  over the alignment score against self, done for all member proteins and averaged. Comparisons of the same protein against itself were omitted from the latter as they would otherwise artificially inflate the score. The two quantities are subtracted and multiplied by 100 to yield the Type III association score. A cutoff of 24 was set by comparison with manually curated examples from previous studies.

Thus a gene cluster seen conserved across a limited range of closely related host genomes was downgraded compared to a gene cluster conserved adjacent to type III systems across widely divergent hosts. The cas association score was used to rank all conserved gene families, and only the top-ranking gene families (with a score above 24) were included for further analyses, with lower ranking gene families assumed to be spuriously associated. Gene clusters corresponding to previously confirmed Type III accessory genes [1,12] were included regardless of association score. Graphical representations of the gene neighbourhoods surrounding all surveyed type III modules were then created and significant accessory genes were marked in order to inspect the results visually and individually. In particular, the visualisations were used to gauge operonic context, in order to assess whether the accessory genes appeared to be cotranscribed with core Type III genes or were encoded as separate transcripts.

## 5.2. *Synechocystis* interference assay

The self-replicating conjugative vector pVZ322 and the gentamicin resistance cassette were used for the construction of invader plasmids to check interference activities in *Synechocystis* sp. PCC 6803 as described in [38]. Spacer 2 was selected to derive an appropriate protospacer sequence and the protospacer sequence was fused in frame to the gentamicin resistance (reporter) gene just upstream of its stop codon in both orientations, sense and antisense, respectively. Mean values of conjugation efficiency and standard deviations were calculated by the ratio of the number of conjugants of target plasmids to non-target plasmids in biological triplicates and in parallel for the control plasmid. Interference activity was observed if the conjugation efficiency was  $< 1$ . Conjugation efficiency of the non-target plasmid was set to 1, which corresponds to no interference activity.

## 5.3. Creation of knock-out mutants and transformation of *Synechocystis* 6803

*Synechocystis* sp. PCC 6803 cultures were grown as described [35]. Single gene knock-out mutants of *slr7080-slr7084*, *slr7088* and *slr7091* were generated by integrating a kanamycin resistance cassette into the corresponding loci. The up-

and downstream flanking regions (1,000 base pairs in size each) were amplified via PCR to ensure site-directed integration via homologous recombination. The resistance cassette was placed in between the upstream and downstream flanking regions in vector pUC19 by Gibson assembly. Transformation of 10 mL *Synechocystis* sp. PCC 6803 aliquots was performed as described [35]. Transformants were tested for full segregation of the introduced knock-out via PCR screening.

#### 5.4. *Synechocystis* 6803 conjugation

Plasmids were conjugated into *Synechocystis* sp. PCC 6803 by triparental mating as described in [36] and few variations described in [38]. Briefly, the helper strain *E. coli* J53/RP4 and the donor strain *E. coli* DH5 $\alpha$  with the plasmid of interest are combined to allow the transfer of the RP4 plasmid into the plasmid of interest bearing cells. After the addition of the recipient strain *Synechocystis* sp. PCC 6803, the plasmid of interest is transferred from the *E. coli* donor strain to the cyanobacterial recipient strain by conjugational transfer. 40  $\mu$ L of cell suspension were plated on BG11 agar plates containing 5  $\mu$ g/mL gentamicin. Conjugants were counted after further incubation at 30°C for 2 weeks.

#### 5.5. RNA analysis and hybridization conditions

RNA extraction from 50 ml *Synechocystis* sp. PCC 6803 cultures was performed as described [35] with the variations mentioned in Behler et al. 2018 [38]. 10  $\mu$ g of total RNA per lane were separated on 1.5% denaturing agarose gel (1.5% agarose, 16% formaldehyde, 10% 10 x MOPS-EDTA-sodium acetate (MEN) buffer) and RNA was transferred to Hybond-N+ membranes (Amersham, Germany) with 20 x SSC buffer by capillary blotting overnight. Generation of a CRISPR3 transcript probe and hybridization conditions were performed as described [38].

#### 5.6. Interaction between c4A and *Sulfolobus* CARF proteins

c4A was synthesized by incubation of Cmr- $\alpha$  with ATP and target RNA (WH, QS unpublished). The interaction between c4A and CARF proteins was determined using a UV cross-link assay as described previously [25]. The extent of activation of the *Sulfolobus* CARF proteins by c4A was determined by measuring RNase activity as described previously [25].

#### Acknowledgments

The authors are grateful to all members of the FOR1680 for helpful discussions.

#### Disclosure statement

The authors declare no conflict of interest.

#### Funding

Shiraz A. Shah and Roger A. Garrett were supported by Copenhagen University. Omer S. Alkhnabashi, Juliane Behler, Wolfgang R. Hess and

Rolf Backofen are supported by the German Research Foundation (DFG) program FOR1680 under grants BA 2168/5-2 and HE 2544/8-2. Wenyuan Han and Qunxin She are supported by the Danish Council for Independent Research [DFF-0602-02196, DFF-1323-00330].

#### ORCID

Shiraz A. Shah  <http://orcid.org/0000-0002-4665-577X>  
Wenyuan Han  <http://orcid.org/0000-0002-9636-6415>  
Qunxin She  <http://orcid.org/0000-0002-4448-6669>  
Wolfgang R. Hess  <http://orcid.org/0000-0002-5340-3423>  
Rolf Backofen  <http://orcid.org/0000-0001-8231-3323>

#### References

- Vestergaard G, Garrett RA, Shah SA. CRISPR adaptive immune systems of Archaea. *RNA Biol.* 2014;11:156–167.
- Makarova KS, Wolf YI, Alkhnabashi OS, et al. An updated evolutionary classification of CRISPR-Cas systems. *Nat Rev Microbiol.* 2015;13:722–736.
- Marraffini LA, Sontheimer EJ. CRISPR interference limits horizontal gene transfer in staphylococci by targeting DNA. *Science.* 2008;322:1843–1845.
- Hale CR, Zhao P, Olson S, et al. RNA-guided RNA cleavage by a CRISPR RNA-Cas protein complex. *Cell.* 2009;139:945–956.
- Peng W, Feng M, Feng X, et al. An archaeal CRISPR type III-B system exhibiting distinctive RNA targeting features and mediating dual RNA and DNA interference. *Nucleic Acids Res.* 2015;43:406–417.
- Elmore JR, Sheppard NF, Ramia N, et al. Bipartite recognition of target RNAs activates DNA cleavage by the Type III-B CRISPR-Cas system. *Genes Dev.* 2016;30:447–459.
- Zhang J, Graham S, Tello A, et al. Multiple nucleic acid cleavage modes in divergent type III CRISPR systems. *Nucleic Acids Res.* 2016;44:1789–1799.
- Han W, Li Y, Deng L, et al. A type III-B CRISPR-Cas effector complex mediating massive target DNA destruction. *Nucleic Acids Res.* 2017;45:1983–1993.
- Tamulaitis G, Venclovas Č, Siksnys V. Type III CRISPR-cas immunity: major differences brushed aside. *Trends Microbiol.* 2017;25:49–61.
- Haft DH, Selengut J, Mongodin EF, et al. A guild of 45 CRISPR-associated (Cas) protein families and multiple CRISPR/Cas subtypes exist in prokaryotic genomes. *PLoS Comput Biol.* 2005;1:e60.
- Makarova KS, Haft DH, Barrangou R, et al. Evolution and classification of the CRISPR-Cas systems. *Nat Rev Microbiol.* 2011;9:467–477.
- Makarova KS, Anantharaman V, Grishin NV, et al. CARF and WYL domains: ligand-binding regulators of prokaryotic defense systems. *Front Genet.* 2014;5:102.
- Zhang J, Rouillon C, Kerou M, et al. Structure and mechanism of the CMR complex for CRISPR-mediated antiviral immunity. *Mol Cell.* 2012;45:303–313.
- Lintner NG, Kerou M, Brumfield SK, et al. Structural and functional characterization of an archaeal clustered regularly interspaced short palindromic repeat (CRISPR)-associated complex for antiviral defense (CASCADE). *J Biol Chem.* 2011;286:21643–21656.
- Zhu X, Ye K. Crystal structure of Cmr2 suggests a nucleotide cyclase-related enzyme in type III CRISPR-Cas systems. *FEBS Lett.* 2012;586:939–945.
- Deng L, Garrett RA, Shah SA, et al. A novel interference mechanism by a type IIIB CRISPR-Cmr module in *Sulfolobus*. *Mol Microbiol.* 2013;87:1088–1099.
- Hatoum-Aslan A, Maniv I, Samai P, et al. Genetic characterization of antiplasmid immunity through a type III-A CRISPR-Cas system. *J Bacteriol.* 2014;196:310–317.



18. Makarova KS, Anantharaman V, Aravind L, et al. Live virus-free or die: coupling of antiviral immunity and programmed suicide or dormancy in prokaryotes. *Biol Direct*. 2012;7:40.
19. Kim YK, Kim Y-G, Oh B-H. Crystal structure and nucleic acid-binding activity of the CRISPR-associated protein Csx1 of *Pyrococcus furiosus*. *Proteins*. 2013;81:261–270.
20. Niewoehner O, Jinek M. Structural basis for the endoribonuclease activity of the type III-A CRISPR-associated protein Csm6. *RNA*. 2016;22:318–329.
21. Yan X, Guo W, Yuan YA. Crystal structures of CRISPR-associated Csx3 reveal a manganese-dependent deadenylation exoribonuclease. *RNA Biol*. 2015;12:749–760.
22. Topuzlu E, Lawrence CM. Recognition of a pseudo-symmetric RNA tetranucleotide by Csx3, a new member of the CRISPR associated Rossmann fold superfamily. *RNA Biol*. 2016;13:254–257.
23. Kazlauskienė M, Kostiuik G, Venclovas Č, et al. A cyclic oligonucleotide signaling pathway in type III CRISPR-Cas systems. *Science*. 2017;357:605–609.
24. Niewoehner O, Garcia-Doval C, Rostøl JT, et al. Type III CRISPR-cas systems produce cyclic oligoadenylate second messengers. *Nature*. 2017;548:543.
25. Han W, Pan S, López-Méndez B, et al. Allosteric regulation of Csx1, a type IIIB-associated CARF domain ribonuclease by RNAs carrying a tetraadenylate tail. *Nucleic Acids Res*. 2017;45:10740–10750.
26. Makarova KS, Grishin NV, Shabalina SA, et al. A putative RNA-interference-based immune system in prokaryotes: computational analysis of the predicted enzymatic machinery, functional analogies with eukaryotic RNAi, and hypothetical mechanisms of action. *Biol Direct*. 2006;1:7.
27. Shmakov S. Systematic prediction of genes functionally linked to CRISPR-Cas systems by gene neighborhood analysis. *PNAS*. 2018;115:E5307–E5316.
28. Enright AJ, Van Dongen S, Ouzounis CA. An efficient algorithm for large-scale detection of protein families. *Nucleic Acids Res*. 2002;30:1575–1584.
29. Punta M, Coggill PC, Eberhardt RY, et al. The Pfam protein families database. *Nucleic Acids Res*. 2012;40:D290–301.
30. Burley SK, Berman HM, Kleywegt GJ, et al. Protein Data Bank (PDB): the single global macromolecular structure archive. *Methods Mol Biol*. 2017;1607:627–641.
31. Staals RHJ, Agari Y, Maki-Yonekura S, et al. Structure and activity of the RNA-targeting Type III-B CRISPR-Cas complex of *Thermus thermophilus*. *Mol Cell*. 2013;52:135–145.
32. Benda C, Ebert J, Scheltema RA, et al. Structural model of a CRISPR RNA-silencing complex reveals the RNA-target cleavage activity in Cmr4. *Mol Cell*. 2014;56:43–54.
33. Hale CR, Cocozaki A, Li H, et al. Target RNA capture and cleavage by the Cmr type III-B CRISPR-Cas effector complex. *Genes Dev*. 2014;28:2432–2443.
34. Shah SA, Erdmann S, Mojica FJM, et al. Protospacer recognition motifs: mixed identities and functional diversity. *RNA Biol*. 2013;10:891–899.
35. Hein S, Scholz I, Voß B, et al. Adaptation and modification of three CRISPR loci in two closely related cyanobacteria. *RNA Biol*. 2013;10:852–864.
36. Scholz I, Lange SJ, Hein S, et al. CRISPR-Cas systems in the cyanobacterium *Synechocystis* sp. PCC6803 exhibit distinct processing pathways involving at least two Cas6 and a Cmr2 protein. *PLoS One*. 2013;8:e56470.
37. Reimann V, Alkhnbashi OS, Saunders SJ, et al. Structural constraints and enzymatic promiscuity in the Cas6-dependent generation of crRNAs. *Nucleic Acids Res*. 2017;45:915–925.
38. Behler J, Sharma K, Reimann V, et al. The host-encoded RNase E endonuclease as the crRNA maturation enzyme in a CRISPR-Cas subtype III-Bv system. *Nat Rev Microbiol*. 2018.
39. Lange SJ, Alkhnbashi OS, Rose D, et al. CRISPRmap: an automated classification of repeat conservation in prokaryotic adaptive immune systems. *Nucleic Acids Res*. 2013;41:8034–8044.
40. Alkhnbashi OS, Costa F, Shah SA, et al. CRISPRstrand: predicting repeat orientations to determine the crRNA-encoding strand at CRISPR loci. *Bioinformatics*. 2014;30:i489–96.
41. Alkhnbashi OS, Shah SA, Garrett RA, et al. Characterizing leader sequences of CRISPR loci. *Bioinformatics*. 2016;32:i576–85.
42. Bernick DL, Cox CL, Dennis PP, et al. Comparative genomic and transcriptional analyses of CRISPR systems across the genus *Pyrobaculum*. *Front Microbiol*. 2012;3:251.
43. Guo L, Brügger K, Liu C, et al. Genome analyses of Icelandic strains of *Sulfolobus islandicus*, model organisms for genetic and virus-host interaction studies. *J Bacteriol*. 2011;193:1672–1680.
44. You X-Y, Liu C, Wang S-Y, et al. Genomic analysis of *Acidianus hospitalis* W1 a host for studying crenarchaeal virus and plasmid life cycles. *Extremophiles*. 2011;15:487–497.
45. Shah SA, Garrett RA. Archaeal type II toxin-antitoxins. In: Kenn Gerdes, editor. *Prokaryotic toxin-antitoxins*. Berlin, Heidelberg: Springer; 2013. p. 225–238.
46. Borges AL, Davidson AR, Bondy-Denomy J. The discovery, mechanisms, and evolutionary impact of anti-CRISPRs. *Annu Rev Virol*. 2017;4:37–59.
47. He F, Bhoobalan-Chitty Y, Van LB, et al. Anti-CRISPR proteins encoded by archaeal lytic viruses inhibit subtype I-D immunity. *Nat Microbiol*. 2018;5(10):018–0120 .
48. Makarova KS, Aravind L, Grishin NV, et al. A DNA repair system specific for thermophilic Archaea and bacteria predicted by genomic context analysis. *Nucleic Acids Res*. 2002;30:482–496.
49. He F, Vestergaard G, Peng W, et al. CRISPR-Cas type IA Cascade complex couples viral infection surveillance to host transcriptional regulation in the dependence of Csa3b. *Nucleic Acids Res*. 2016;45:1902–1913.
50. Liu T, Liu Z, Ye Q, et al. Coupling transcriptional activation of CRISPR-Cas system and DNA repair genes by Csa3a in *Sulfolobus islandicus*. *Nucleic Acids Res*. 2017;45:8978–8992.
51. Sinkunas T, Gasiunas G, Fremaux C, et al. Cas3 is a single-stranded DNA nuclease and ATP-dependent helicase in the CRISPR/Cas immune system. *EMBO J*. 2011;30:1335–1342.
52. Beloglazova N, Petit P, Flick R, et al. Structure and activity of the Cas3 HD nuclease MJ0384, an effector enzyme of the CRISPR interference. *EMBO J*. 2011;30:4616–4627.
53. Westra ER, Van Erp PBG, Künne T, et al. CRISPR immunity relies on the consecutive binding and degradation of negatively supercoiled invader DNA by Cascade and Cas3. *Mol Cell*. 2012;46:595–605.
54. Koonin EV, Makarova KS. Discovery of oligonucleotide signaling mediated by CRISPR-associated polymerases solves two puzzles but leaves an enigma. *ACS Chem Biol*. 2018;13:309–312.
55. Edgar RC. MUSCLE: multiple sequence alignment with high accuracy and high throughput. *Nucleic Acids Res*. 2004;32:1792–1797.
56. Söding J, Biegert A, Lupas AN. The HHpred interactive server for protein homology detection and structure prediction. *Nucleic Acids Res*. 2005;33:W244–8.